

Article citation info:

Zhang X, Li J, Li X, Li Q, Cutting Characteristics and Reliability Analysis of Conical Picks Containing Prefabricated Grooved Rocks, *Eksploracja i Niezawodność – Maintenance and Reliability* 2024; 26(4) <http://doi.org/10.17531/ein/191694>

## Cutting Characteristics and Reliability Analysis of Conical Picks Containing Prefabricated Grooved Rocks

Indexed by:



Xin Zhang<sup>a</sup>, Juntao Li<sup>a</sup>, Xu Li<sup>a,\*</sup>, Qinghai Li<sup>b</sup>

<sup>a</sup> College of Mechanical and Electrical Engineering, Shandong University of Science and Technology, China

<sup>b</sup> Zhuanlongwan Coal Mine, Ordos Energy Company, China

### Highlights

- Analysis of ways to improve rock cutting performance and increase equipment reliability
- Comparative study of rock cutting performance with and without grooves.
- Exploring the effect of groove and pick positional relationship on cutting characteristics.
- Analysis of the specific energy consumption under different cutting parameters.

### Abstract

When a roadheader breaks hard rock in a roadway, the excessive cutting load causes the conical pick to experience abnormal wear, which impacts equipment stability. To improve the reliability of hard rock cutting equipment, the dynamic characteristics of prefabricated grooved rocks during cutting were investigated using a single pick cutting experimental bench in rock crushing experiments, and a conical pick cutting rock breaking finite element model was established. The rock stress state under different cutting depths and spacing conditions was analyzed, and the cutting force and the trend of the change in the specific energy consumption were elucidated. The results show that prefabricated grooves can effectively reduce the cutting load and specific energy consumption, the cutting depth and conical pick–groove spacing are the key factors affecting the cutting characteristics, and a reasonable choice of spacing and depth can help reduce the wear of conical picks and improve the working reliability of roadheaders.

### Keywords

reliability, cutting load, roadheader, conical pick, prefabricated groove

This is an open access article under the CC BY license (<https://creativecommons.org/licenses/by/4.0/>)

### 1. Introduction

Roadheader<sup>[1]</sup> bodies are small, can be moved flexibly, and are more adaptable to the more complex mining environment of coal mines; thus, currently, the roadheader is still the main piece of equipment used for the task of coal mine roadway tunneling. The roadheader penetrates a rock body using a conical pick on a cutting head to break the rock to create the roadway boring. Hard rock crushing is a common problem in the roadheader tunneling process. As shown in Fig. 1, when a conical pick cuts through hard rock, it is subjected to increased cutting loads, resulting in abnormal and increased wear of the conical pick<sup>[2]</sup>.

<sup>3]</sup>. During the rock crushing process, the reaction force increases, the load fluctuates, the roadheader body vibrates abnormally, and the roadheader mechanical connection and transmission parts can shrink, reducing the stability of the roadheader<sup>[4]</sup> and causing it to be prone to tipping and skidding, which seriously affects the reliability of the work of the roadheader. Therefore, this paper proposes the method of prefabricated grooves to increase the free surface of the rock and change its mechanical properties, analyzes the influence of the grooves on the cutting performance of conical picks, and studies the relationship

(\*) Corresponding author

E-mail addresses: X. Zhang [zhangxin@sdust.edu.cn](mailto:zhangxin@sdust.edu.cn), J. Li (ORCID: 0009-0009-0207-1682) [202280050004@sdust.edu.cn](mailto:202280050004@sdust.edu.cn), X. Li (ORCID: 0000-0002-7730-3646) [lixu2017@sdust.edu.cn](mailto:lixu2017@sdust.edu.cn), Q. Li [3208013890@qq.com](mailto:3208013890@qq.com)

between conical picks and the corresponding positions of prefabricated grooves on the cutting characteristics to reduce the cutting load, thereby reducing the wear of conical picks; this study is highly important for improving the efficiency of the rock breaking by roadheaders and the reliability of roadheaders.



Fig. 1. Wear and tear on roadheader conical picks.

Zhao<sup>[5]</sup> et al. investigated the dynamic reliability of drums in terms of load, stress, and wear and showed that as the traction speed increases, the load and stress increase, leading to an increase in the wear of conical picks. Praetzas, C<sup>[6]</sup> et al. investigated the effects of parameters such as tool load on tool life and showed that there is a strong interdependence between tool wear and load. Liu<sup>[7]</sup> et al. investigated the effect of the cutting type on the stress state and load characteristics of rock and showed that the reaction force of rock on the tool mainly leads to tool wear, and the stress state and load characteristics of rock are reflected in the wear condition of the tool. Li<sup>[8]</sup> et al. conducted linear cutting experiments and showed that the cutting load to which the pick is subjected is the main cause of pick wear. These studies have shown that tool wear is influenced mainly by the cutting load. Zhang<sup>[9]</sup> investigated the effect of factors such as structure and operating parameters on the wear performance of a tool, and the results showed that tool wear is mainly affected by the cutting force and that tip wear reduces the ability of the tool to cut the rock. Sun<sup>[10]</sup> et al. showed through rock-cutting experiments that a worn tool significantly affects the cutting force as well as the rock-breaking effect, and the tool is subjected to high loads during tool wear. Dogruoz, C<sup>[11]</sup> et al. conducted full-size cutting experiments using drills with different levels of wear and showed that drill wear leads to

an increase in cutting force and specific energy consumption, which is detrimental to cutting stability. Tool wear has an impact on the effectiveness of rock breaking and is detrimental to the reliable operation of equipment.

Wang<sup>[12]</sup> et al. investigated the influence of cutting parameters on cutting force and rock damage by establishing a numerical model of rock cutting with a conical pick. Wang<sup>[13]</sup> et al. performed conical pick-cutting experiments and showed that cutting depth and line spacing have significant effects on rock cutting. By analyzing the stress and damage trends, Jiang<sup>[14, 15]</sup> et al. showed that the formation of crushed zones, large debris, and cracks are closely related to the contact force. These studies analyzed the mechanism of tool rock breaking and the changes in load and energy consumption via numerical simulations and experiments. Some scholars have also researched new rock-breaking methods, such as lasers<sup>[16, 17]</sup>, plasma<sup>[18]</sup>, and microwaves<sup>[19]</sup>, but these methods are difficult to apply due to the high-gas environment of coal mines.

Yang<sup>[20]</sup> et al. conducted uniaxial compression tests on prefabricated grooved rock specimens and monitored and analyzed the damage process, revealing the relationship between crack extension and stress changes in groove-containing rocks. Ping<sup>[21]</sup> et al. conducted impact compression tests on fracture-bearing sandstones and analyzed the effect of fracture on the fragmentation shape, dynamic compressive strength, and energy consumption of rock. Huang<sup>[22]</sup> et al. carried out a numerical simulation of defective rock specimens to analyze the cracking process and stress-strain change rule. Li<sup>[23]</sup> et al. conducted compression damage experiments on rocks containing prefabricated grooves and showed that the stress direction plays a very important role in inducing rock crack extension. These studies show that the free surface can weaken the mechanical properties of the rock, making the rock more fragile. Li<sup>[24]</sup> et al. proposed different forms of prefabricated groove-assisted rock-breaking models and showed that the grooves induced crack development and helped to reduce the specific energy and cutting force. Wang<sup>[25]</sup> et al. analyzed the influence of prefabricated grooves on the cutting characteristics of PDC tools and showed that increasing the groove depth and number can reduce the cutting force, increase the quality of rock fragmentation and improve the crushing efficiency. Zhang<sup>[26]</sup> et al. investigated the effect of

prefabricated notches on the rock fragmentation process based on a discrete element numerical model and analyzed the relationships among the cutting depth, notching parameters, and rock fragmentation properties. Lu<sup>[27]</sup> et al. built a water jet rock-breaking test bed to analyze the cutting depth of a high-pressure water jet and the cutting angle of a TBM hob, and they showed that a groove depth deeper than the penetration depth is more conducive to rock breaking. There are two main methods for producing prefabricated grooves in rock: abrasive water jets and sawing. The abrasive water jet method generates grooves by using high-pressure water containing abrasive particles to impact and shear rocks at high speeds. Sawing is the process of cutting grooves through contact between a high-speed rotating saw blade and rock under external forces. Both methods are suitable for the coal mine tunnel environment; therefore, this study chose the sawing method to produce prefabricated grooves in rocks. At present, underground rock-breaking tools for coal mines are still dominated by conical picks, but there are few studies on the performance of conical picks in crushing rocks with prefabricated grooves, so there is a need for relevant research on conical picks.

To improve the working reliability of roadheaders in rock crushing, this paper studies the cutting characteristics of prefabricated groove rocks, builds a single pick cutting rock test bench, carries out rock crushing experiments, analyzes the cutting load and rock crushing state, establishes a numerical

model of rock crushing by conical pick, and determines the stress distribution of rock. Combining experimental and numerical analyses, the influence of the cutting depth and pick-groove spacing on the cutting load and cutting specific energy consumption are investigated, which are highly important for improving the efficiency of hard rock crushing in coal mine roadheaders, reducing the energy consumption of cutting, and ensuring the working reliability of roadheaders.

## 2. Methods and models

### 2.1. Experimental program design

#### 2.1.1. Experimental setup

The single pick-cutting rock test bench built in this paper is shown in Fig. 2 and is mainly composed of a hydraulic power part, a rock-cutting part, and a test signal acquisition part. The hydraulic power part, which provides speed and propulsion for conical pick cutting, includes a hydraulic pump station and hydraulic cylinder; the rock cutting part includes a conical pick, rock clamping platform, moving guide column, and conical pick nudge plate to ensure the stability of conical pick traveling during the cutting process; and the test signal acquisition part, which consists of a three-way force sensor, a displacement sensor, and a signal acquisition system, is used to collect the force signals generated in the cutting process.

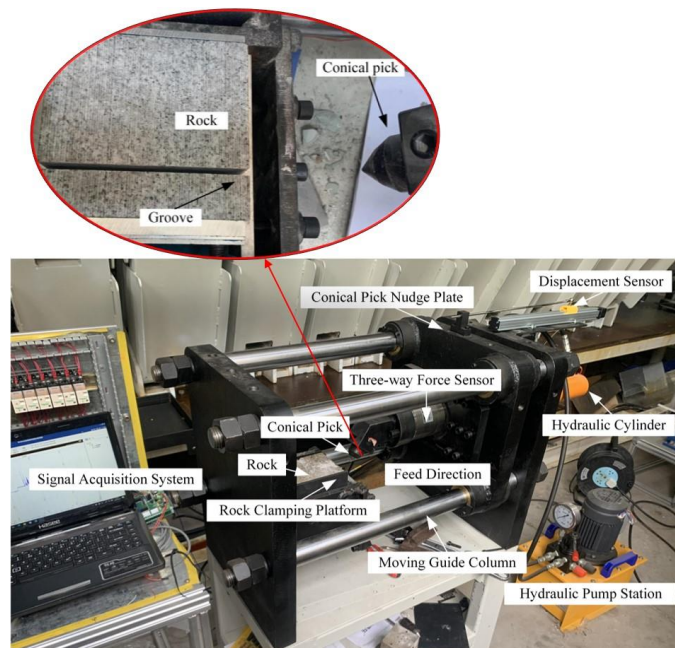


Fig. 2. Single pick cutting rock test bench.

### 2.1.2. Experimental program

This experiment was conducted with three groups using the controlled variable method. The first group consists of groove-free rock-cutting experiments to investigate the effects of different cutting depths on the rock-breaking process of the conical draft by varying the cutting depth ( $h$ ). The second group consists of cutting experiments on rocks with prefabricated grooves, determines the cutting depth ( $h=12$  mm), changes the conical pick-groove spacing ( $s$ ), and explores how different conical pick groove spacings under the same cutting depth affect the force. The third group of experiments determines the conical pick-groove spacing ( $s=9$  mm), changes the cutting depth ( $h$ ), explores how rock containing prefabricated grooves of different cutting depths affect the force, and compares the results with those of the first group of experiments to analyze the effect of having prefabricated grooves on the cutting force

under the same cutting depth. The rock debris from all the above experiments was also collected, weighed, and statistically analyzed to determine the cutting specific energy consumption. The variable parameters were set as shown in Table 1:

Table 1. Parameter list of variables.

Group	cutting depth $h$ (mm)	conical pick-groove spacing $s$ (mm)
1	6, 9, 12, 15	\
2	12	3, 6, 9, 12
3	6, 9, 12, 15	9

### 2.2. Model of rock cutting by conical picks

The relative relationship between the conical pick and the rock is shown in Fig. 3, where  $v$  is the feeding direction of the conical pick, the half-cone angle of the tip of the conical pick is  $38^\circ$ , the cutting angle between the conical pick and the rock is  $45^\circ$ , and the rock dimensions are 140 mm in length, 130 mm in width and 110 mm in height.

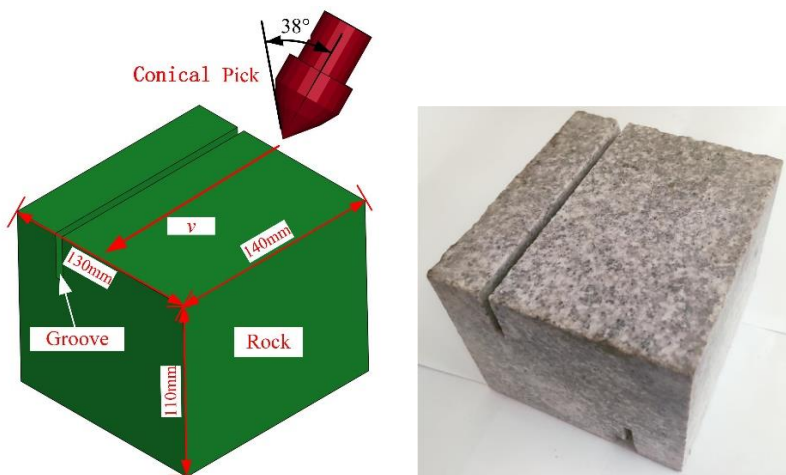


Fig. 3. Model of rock cutting using a conical pick.

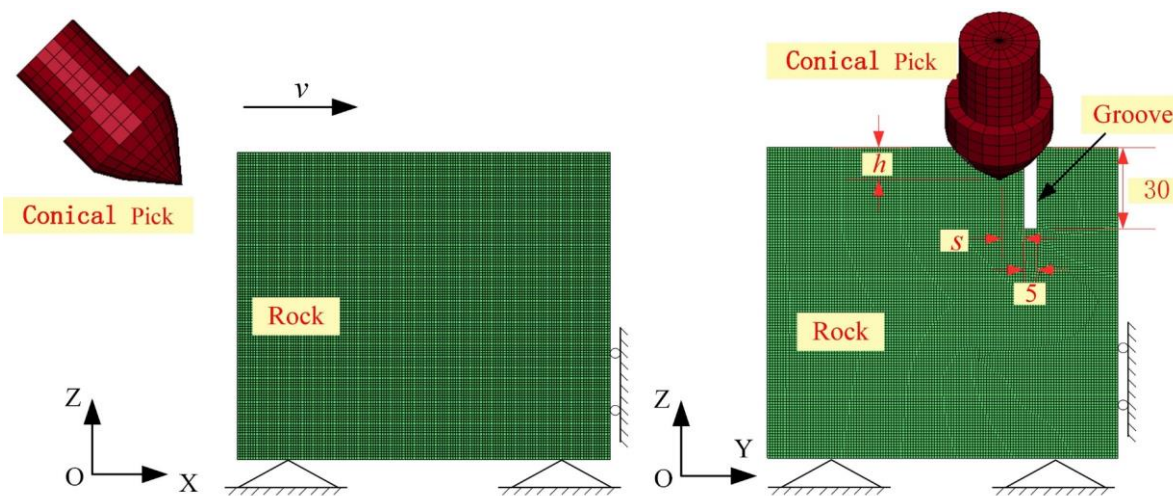


Fig. 4. Finite element modeling diagram of rock cutting by conical picks.

Fig. 4 shows the finite element model diagram of rock cutting by conical pick, where  $h$  is the cutting depth and  $s$  is the conical pick–groove spacing. Under actual working conditions, the volume of the rock is large compared to that of the conical pick, the side and bottom of the rock are set up to simulate the nonreflective boundary conditions, the bottom of the rock is set up with full constraints, and the tool only retains the degrees of freedom in the feed direction and restricts the motion in other directions<sup>[28]</sup> to avoid offset cutting of the rock by the tool. The conical pick makes direct contact with the rock to break the rock, and the numerical analysis in this paper mainly studies the stress condition of the conical pick and the rock and the stress distribution law of the rock. A total of 200200 rock cells and 1500 conical pick cells were generated by dividing the rock model using 1 mm hexahedral meshes<sup>[29]</sup> and rotationally dividing the conical picks using 3 mm meshes. It is ensured that sufficient cells exist in the finite element model to participate in the simulation calculation at the minimum cutting depth ( $h=6$  mm) and the minimum pick–groove spacing ( $s=3$  mm).

### 2.3. Ontological modeling of rock materials

Holmquist–Johnson–Cook (HJC) materials are often used to simulate the rock crushing process<sup>[30]</sup>. HJC materials are concrete damage material models that can accurately reflect the dynamic response of high strain and large deformation damage failure, have excellent performance in simulating the mechanical properties and crushing morphology of rocks and other materials, and can be better applied to rock cutting and crushing processes with large load fluctuations. The HJC intrinsic model consists of three main aspects: the strength equation, the state equation, and the damage evolution equation.

The yield strength equation for the HJC model is given in Equation (1):

$$\sigma^* = [A(1-D) + BP_1^N][1 + C(\ln \dot{\epsilon}^*)] \quad (1)$$

where  $\sigma^*$  is the standardized equivalent stress;  $A$  is the standardized cohesion strength;  $D$  is the damage coefficient;  $B$  is the standardized pressure strengthening coefficient;  $P^*$  is the standardized hydrostatic pressure;  $N$  is the pressure hardening coefficient;  $C$  is the strain rate coefficient; and  $\dot{\epsilon}^*$  is the dimensionless strain rate.

The state equation for the HJC material is as follows.

When  $P \leq P_c$ , as shown in Equations (2) and (3),

$$P = K\mu \quad (2)$$

$$K = P_c/\mu_c \quad (3)$$

where  $P$  is the hydrostatic pressure of the material;  $K$  is the bulk elastic modulus of the material;  $P_c$  is the critical pressure of the material when the voids start to close;  $\mu_c$  is the corresponding bulk strain;  $\mu = (\rho/\rho_0) - 1$  is the volumetric strain of the cell; and  $\rho/\rho_0$  are the real-time and initial densities of the cell, respectively.

When  $P_c \leq P \leq P_l$ , the fracture cracks in the rock start to form, which are expressed as Equation (4) and Equation (5).

$$P = P_c + K_c(\mu - \mu_c) \quad (4)$$

$$K_c = (P_l - P_c)/(\mu_l - \mu_c) \quad (5)$$

where  $\mu_l$  is the corresponding volumetric strain, and  $P_l$  is the compaction hydrostatic pressure.

When  $P > P_l$ , the rock is fully compacted, as expressed in Equation (6):

$$P = D_1\bar{\mu} + D_2\bar{\mu}^2 + D_3\bar{\mu}^3 \quad (6)$$

where  $\bar{\mu}$  is the modified volumetric strain and  $D_1$ ,  $D_2$ , and  $D_3$  are pressure constants.

The accumulation of equivalent plastic strain and plastic volumetric strain leads to model damage, which is given by the damage equation shown in Equation (7):

$$D = \sum \frac{\Delta \epsilon_p + \Delta \mu_p}{\epsilon_p^f + \mu_p^f} \quad (7)$$

where  $\Delta \epsilon_p$  is the equivalent plastic strain increment of the unit in one calculation cycle;  $\Delta \mu_p$  is the plastic volume increment of the unit in one calculation cycle;  $\epsilon_p^f$  is the equivalent plastic strain of crushing at atmospheric pressure; and  $\mu_p^f$  is the equivalent plastic volumetric strain of crushing at atmospheric pressure.

The rock material used in this paper is granite, and the mechanical parameters are shown in Table 2.

Table 2 Rock material parameters

Density (kg/m <sup>3</sup> )	Modulus of elasticity(MPa)	Poisson's ratio	Tensile strength(MPa)	Compressive strength(MPa)
2670	2.8E4	0.3	9.8	121.2

When the conical pick cuts the rock, the force on the conical pick is divided into three directions of force along the X, Y, and Z directions, as shown in in Fig. 4, where the X-axis direction is defined as the feed force and the Y-axis direction is the lateral force. Finite element simulation analysis is carried out using the same parameters as the test, and the stress distribution state of the rock during the conical pick-cutting process can be obtained through numerical analysis, which is used to analyze the mechanism by which the prefabricated grooved rocks enable

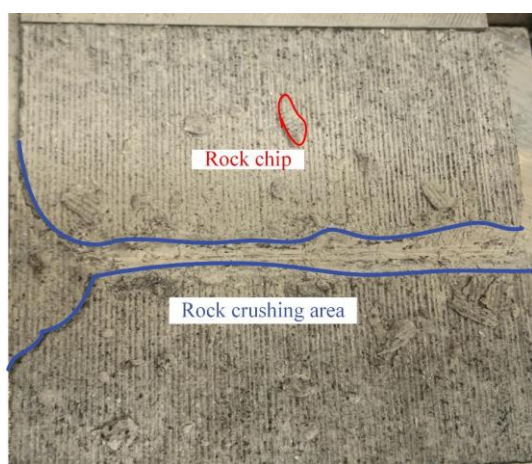
crushing under the action of conical pick cutting.

### 3. Analysis and discussion of the cutting characteristics

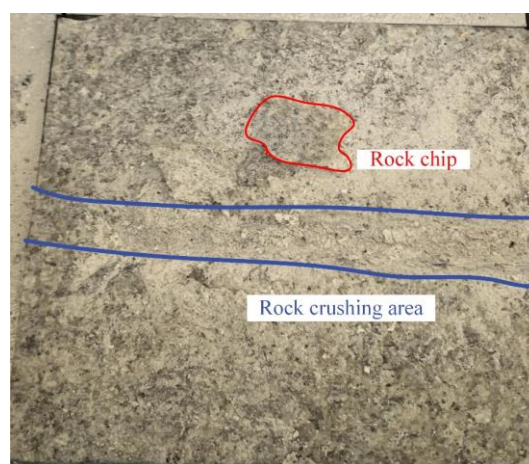
#### 3.1. Prefabricated groove-free rock cutting analysis

Fig. 5 shows the graph of the crushing state of groove-free rocks with different cutting depths. As the cutting depth increases, the crushing area of the rock gradually increases horizontally and vertically, and the amount of the generated rock chips also increases. Due to the increasing distance of the conical pick tip from the upper surface of the rock, the rock is extruded by the intrusion of the pick tip to produce a dense core, and the cracks produced when the dense core is released need to be extended to the free surface to cause the rock mass to flake. When the

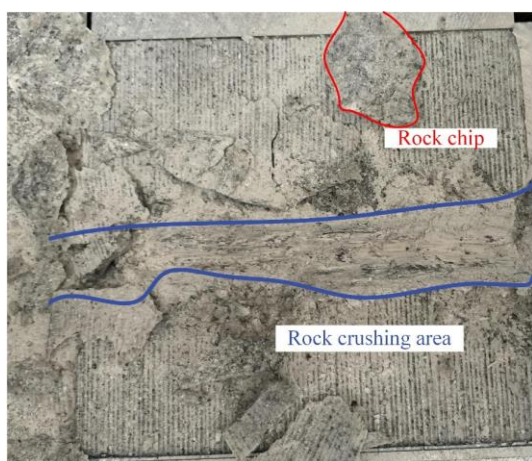
cutting depth is shallow, the cracks produced by the release of the dense core spread in all directions, and because of the proximity to the upper surface, the cracks have a small radius of extension, thus producing small rock chips and a smaller crushing area; when the cutting depth is deeper, the cracks produced by the release of the dense core have spread out by the time they reach the upper surface, producing larger rock chip chunks and a larger crushing area. When the cutting depth is 15 mm, the crack extension radius released by the dense core is smaller than the cutting depth, and most of the cracks cannot extend to the upper surface, so the rock chips produced by rock crushing are large in size but small in number.



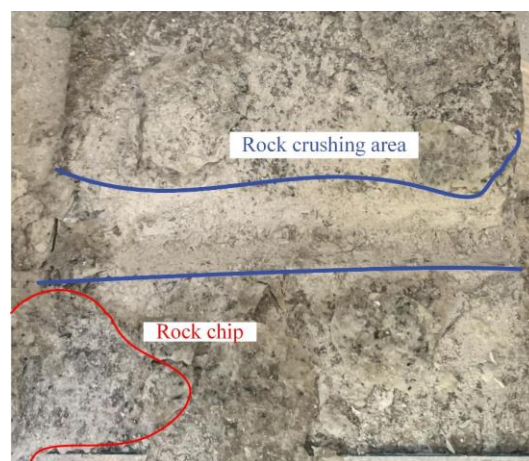
(a)  $h=6$  mm



(b)  $h=9$  mm



(c)  $h=12$  mm



(d)  $h=15$  mm

Fig. 5. Diagram of the crushing state of groove-free rocks with different cutting depths.

The stress distribution state of the groove-free rock is shown in Fig. 6. With increasing cutting depth, the area affected by the rock force gradually increases, the stress concentration is generated at the tip of the pickaxe, the rock is completely

crushed through contact with the tip of the pickaxe, and the stress expands from the tip of the pickaxe to the free surface, which is consistent with the trend of crack extension generated in the rock crushing process.

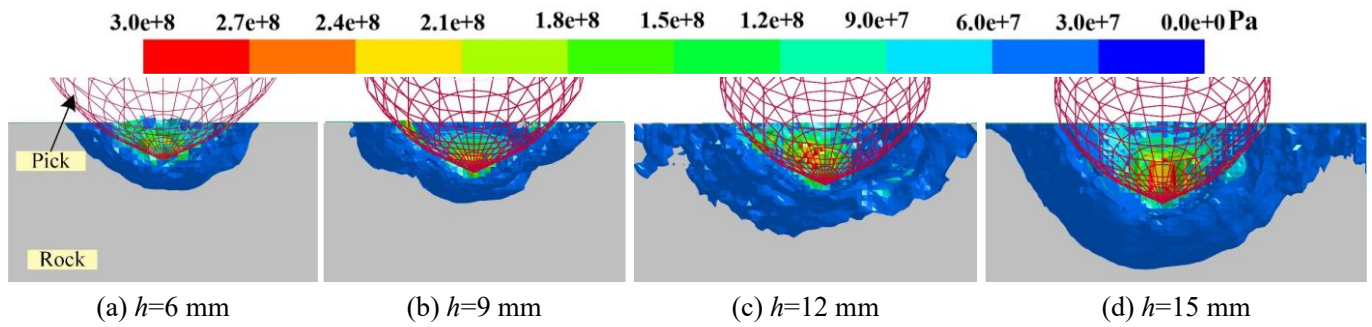


Fig. 6. Stress distribution cloud map of a groove-free rock.

Fig. 7 shows the feed force curves for different cutting depths of groove-free rock. The feed force curve exhibits jagged fluctuations over time. The same feed force curve first increases at a very fast rate, reaches a peak value, and then decreases rapidly, reflecting the characteristics of a rock step fracture, which is consistent with the process of continuous formation and release of the dense core. In addition, comparing the simulation curves, the fluctuation amplitude of the feed force curves of the experiment with all samples having the same cutting depth is larger, which is due to the inhomogeneity of the internal structure of the rock, the randomness of the crack extension, and the different size of the spalled rock, so the feed resistance peak of the conical pick is different. The coefficient

of variation is a relative statistic that measures the degree of variability of the data and is commonly used to compare the degree of data dispersion; it is the ratio of the standard deviation to the mean, which eliminates the effect of differences in the mean values of the data on the evaluation of volatility and therefore provides a better reflection of load fluctuations. The coefficient of variation of rock cutting increases from 0.29 to 0.57 when the cutting depth increases from 6 mm to 15 mm. When the cutting depth is shallow, the crack easily extends to the upper free surface, and the cutting is smoother; when the cutting depth is greater, it is more difficult for the crack to extend to the free surface, the cutting force fluctuates more, and the equipment cutting stability is reduced.

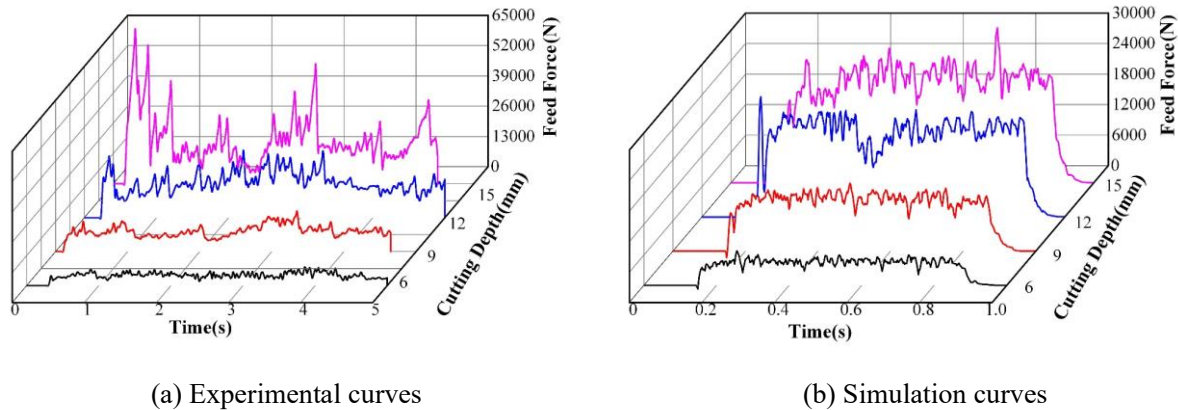
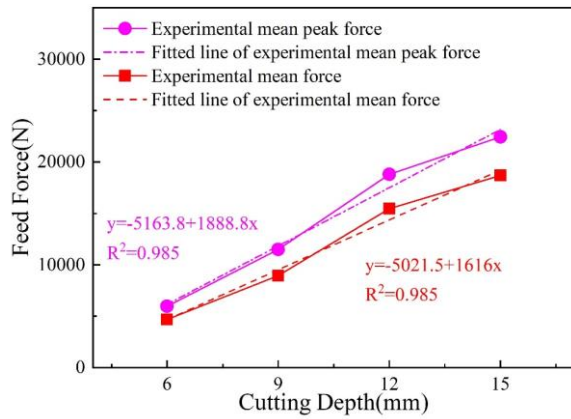


Fig. 7. Feed force curves for different cutting depths of groove-free rock.

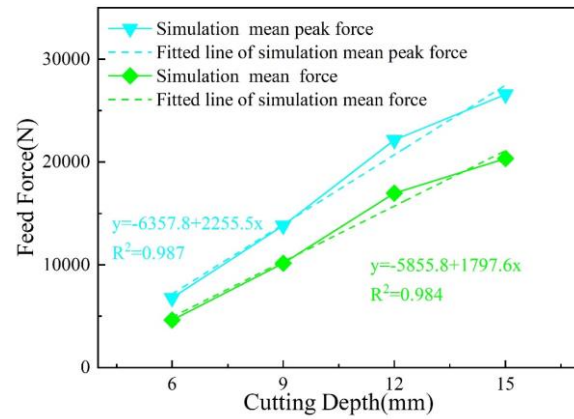
The aggregation of energy in the rock near the tip of the pick, accompanied by the release of energy from fragmentation of the rock mass, leads to fluctuations in the cutting loads. The peak cutting force is the force on the conical pick at the moment when the rock breaks under the extrusion of the pick tip. To carry out a more accurate quantitative analysis of the cutting process, the law of change of the cutting force in the cutting process was studied, and the statistical analysis of the mean peak force was performed.

As shown in Fig. 8, when the cutting depth is 6 mm, the

mean peak force obtained by the experiment is 5976 N, and that of the simulation data is 6798 N. When the cutting depth is 15 mm, the experimental mean peak force is 22427 N, and that of the simulation experiment can reach 26570 N. With increasing cutting depth, the mean value of the feed force and the mean peak force tended to increase. Linear fitting of the obtained mean value of the feed force as well as the mean peak force reveals that the preformed groove-free feed force shows a strong linear relationship with the cutting depth.



(a) Experimental data



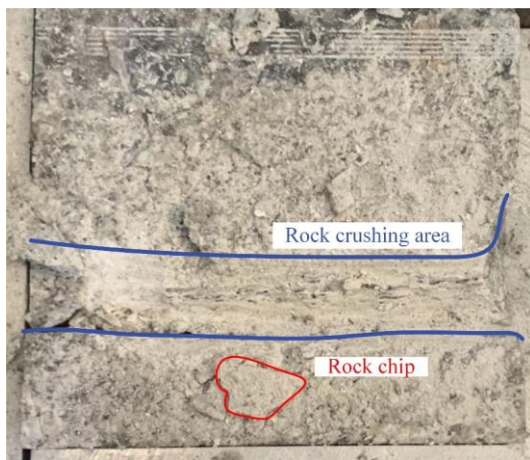
(b) Simulation data

Fig. 8. Statistical graph of the feed force for different cutting depths in groove-free rock.

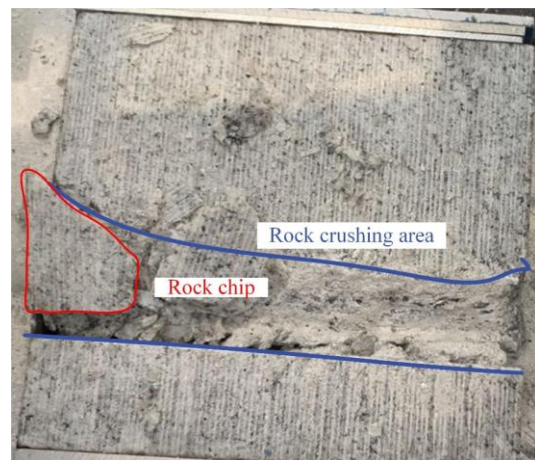
### 3.2. Analysis of rock cutting with different conical pick-groove spacings

Fig. 9 shows the rock fragmentation state with different pick-groove spacings, analyzed for a cutting depth of 12 mm and conical pick-groove spacing ratios of 3 mm, 6 mm, 9 mm, and 12 mm. The rock crushing area changes with the conical pick position, the crushing area continues to increase with increasing spacing, the amount of rock debris cut by the conical pick increases, the amount of debris biased to the side of the groove increases, and the rock avalanche angle increases. In the case of a conical pick that cracks at the tip of the pick while cutting groove-containing rock, the grooves provide a free surface for the cracks to extend, the groove side of the rock is more easily spalled, and the rock debris is biased toward the groove side. As the pick-groove spacing increases, the extension distance from the cracks to the free surface at the grooves gradually increases, only the larger cracks extend to the free surface, the chipping

angle increases continuously, and the rock fragmentation generates a corresponding increase in the lumpiness of the rock chips. Fig. 10 shows the stress distribution of the rock. When the pick-groove spacing is small, the stress is distributed on both sides of the groove, concentrating on the pick-tip side and extending along the upper free surface on both sides, and as the distance of the pick tip from the groove increases, the stress extends downward along the free surface provided by the groove, and the range of stress increases. The presence of the groove blocks the transfer of stresses, and the rock will fail at the groove location under the cutting action of the conical pick when the pick tip is near the groove location. When the pick tip is far from the groove, the cracks produced by rock crushing will follow the direction of stress extension and extend downward along the groove, and with increasing conical pick-groove spacing, the stress-affected area and the rock crushing area will both deepen.



(a)  $s=3$  mm



(b)  $s=6$  mm

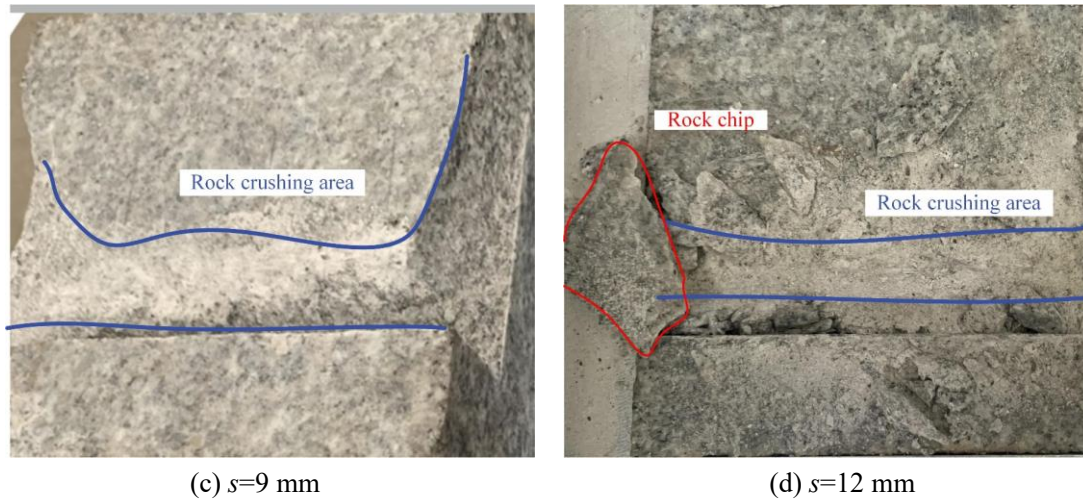


Fig. 9. Diagram of the rock fragmentation state with different conical pick-groove spacings.

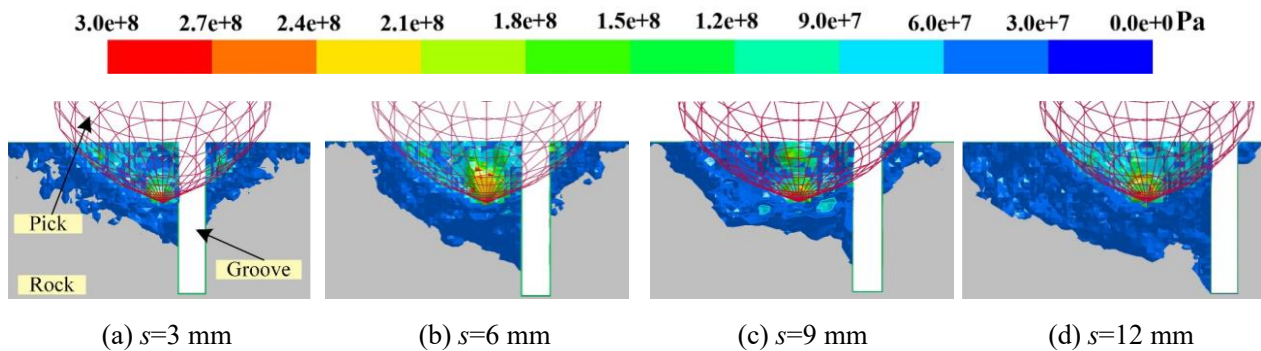


Fig. 10. Stress distribution of rocks with different conical pick-groove spacings.

As shown in the feed force graph of Fig. 11, the fluctuations in the feed force during the experiment shows are larger than those of the simulation data. The feed force was statistically analyzed by comparing groove-free rocks with the same cutting depth, as shown in Fig. 12. The feed force increased continuously with increasing pick-groove spacing, but the increase was smaller and levelled off in the later stages, and the feed force values of all of the samples were smaller than the feed force of the groove-free rock at the same cutting depth. This is because the groove provides a new free surface for crack

expansion, reduces the difficulty of rock crushing, reduces the feed force of rock crushing, and improves the reliability of cutting and breaking rock when working. As the pick-groove spacing increases, the cracks produced during rock crushing extend to the free surface of the groove at an ever-increasing distance, and the area of contact between the pick and the rock increases, resulting in an increasing cutting volume, an increase in the lumpiness of the rock debris, and an increase in the feed force.

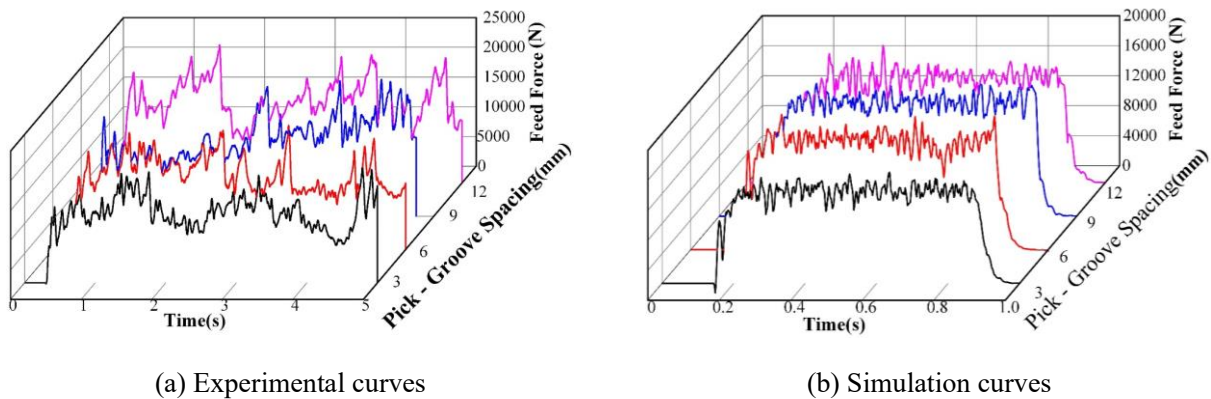
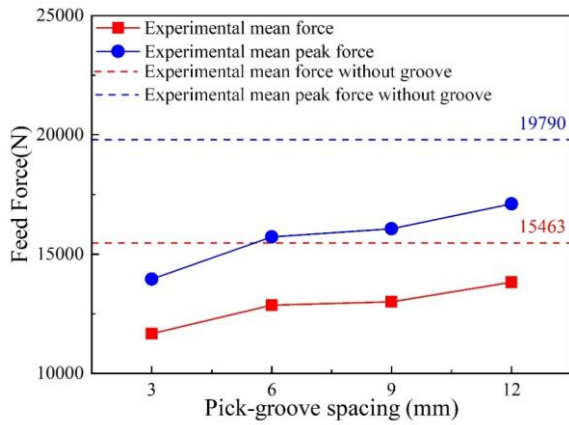
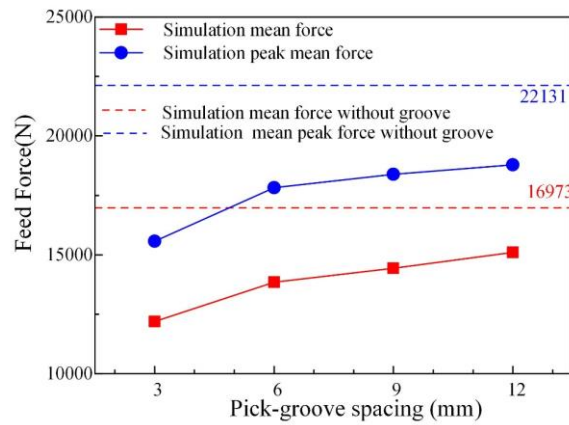


Fig. 11. Feed force curves for different conical pick-groove spacings.



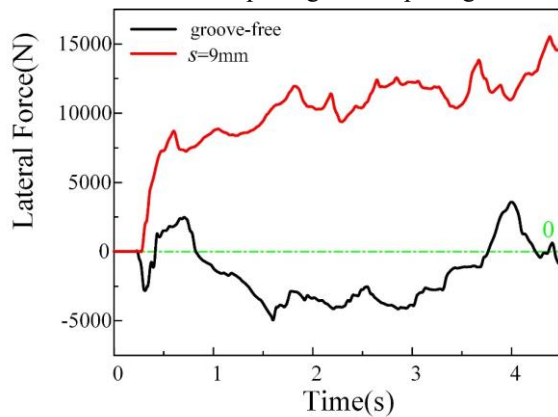
(a) Experimental data



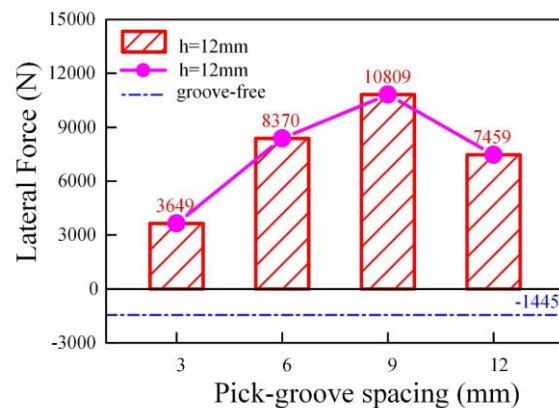
(b) Simulation data

Fig. 12. Statistical graph of the feed force for different conical pick-groove spacings.

Fig. 13(a) shows the comparison of lateral force curves for groove-free rock and a pick-groove spacing of 9 mm for a cutting depth of 12 mm. The lateral force amplitude during the crushing of groove-free rock is low and fluctuates on both sides above and below zero, whereas during the crushing of groove-containing rock, the lateral force is biased toward the side of the groove due to the presence of the groove, which provides a new free surface. Fig. 13(b) shows the statistical plot of the mean lateral force values for different pick-groove spacings. The



(a) Lateral force curves ( $s=9$  mm)



(b) Average value of lateral forces

Fig. 13. Comparison of lateral force statistics for different pick-groove spacings.

### 3.3. Analysis of rock cutting in prefabricated grooves at different cutting depths

Fig. 14 shows a graph of the rock fragmentation state at different cutting depths for a pick-groove spacing of 9 mm. As the cutting depth increases, the crushed area of the rock expands, and the rock debris increases in size and becomes more concentrated on one side of the groove. Fig. 15 shows the stress distributions with different cutting depths of groove-containing rocks, and the maximum stress occurs at the tip of the pick. With increasing cutting depth, the stress area increases, but it is

lateral force increases and then decreases with increasing spacing because at closer spacings, the crack extension to the free surface at the groove is also closer, and rock spalling can occur under a smaller lateral force. The decrease in the mean lateral force at a conical pick-groove spacing of 12 mm occurs because as the spacing increases, the free surface provided at the groove has less influence on crack extension, and some of the lateral force is directed toward the rock side and is not just singularly biased toward the groove side.

smaller than that of the groove-free rock at the same cutting depth. When the cutting depth is small, the grooves block the transfer of stress, and the stress tends to be distributed on the side of the groove and extends. Cracks are generated by the pick tip. On the side near the groove, due to the distance between the tip of the conical pick and the free surface being less, the newly generated cracks expand along a shorter path. Due to the presence of the groove, the rock undergoes a certain amount of stretching under the extrusion of the pick, which is more prone to fracture, so the rock on the side near the free surface crumbles

under the action of less stress. On the groove-free side, due to the long path from the groove, it can only be extended to the upper free side to flake the rock mass, and rock crushing is more difficult. Therefore, the rock debris is heavily concentrated on the groove side. With increasing cutting depth, cracks occur at

greater depths, only larger cracks expand to the free surface, the amount of energy increases, the amount of rock crushing that generates the block size of the rock debris increases accordingly, the rock crushing area increases, and the stability of the equipment decreases.

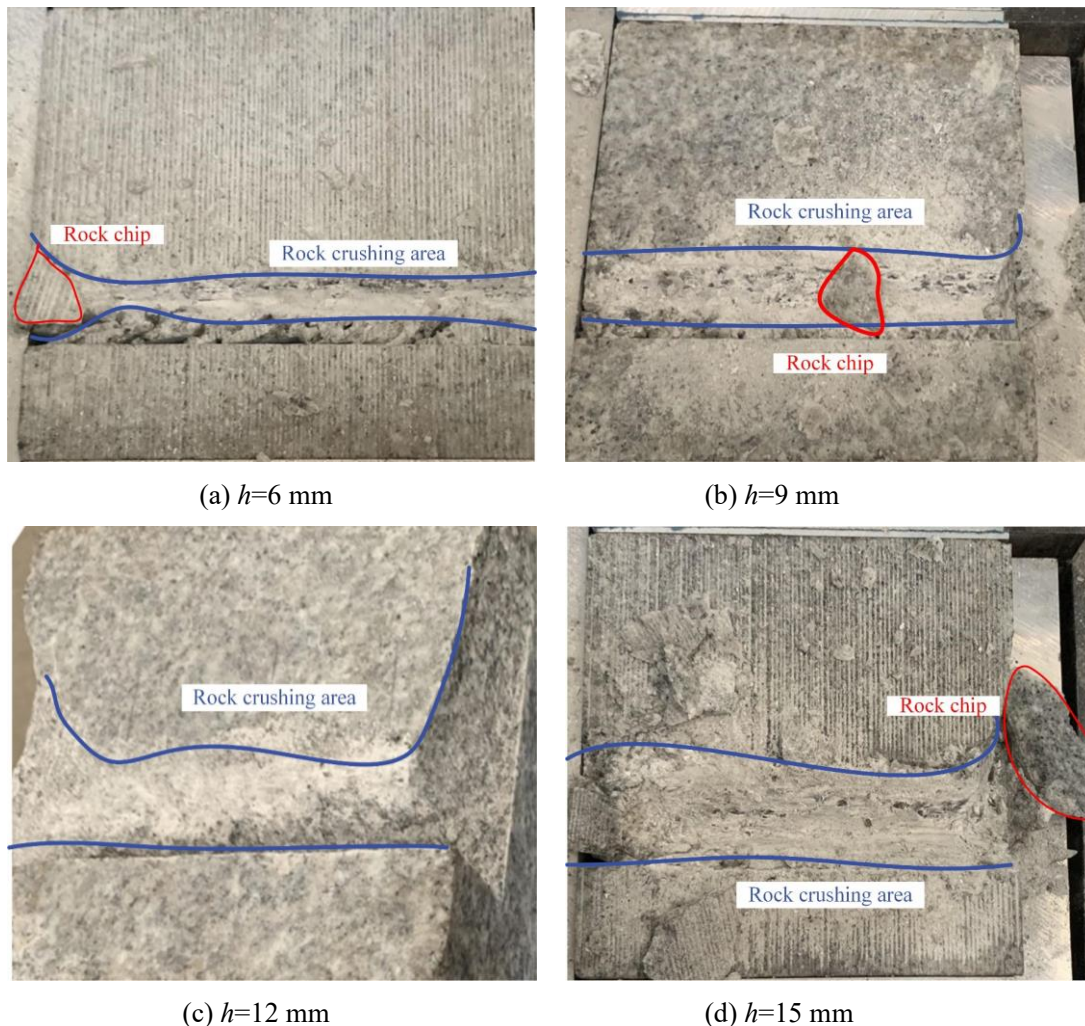


Fig. 14. Diagram of the crushing state of groove-containing rocks with different cutting depths.

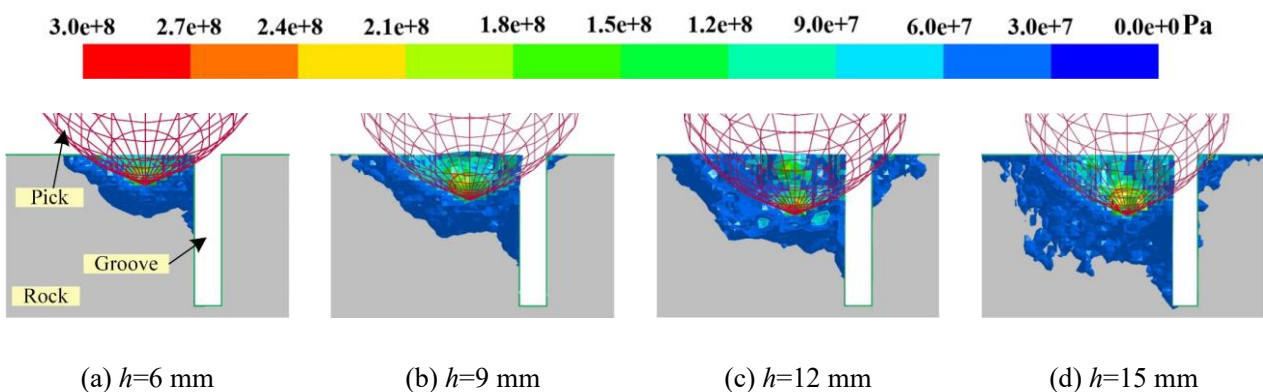


Fig. 15. Rock stress distributions of groove-bearing rocks with different cutting depths.

Fig. 16 shows the cutting force curves for different cutting depths of groove-containing rocks. Compared with the groove-free cutting force curve, the curve fluctuation is smaller, and the

maximum value of the groove-containing feed force is 25000 N in the experimental data, which is much smaller than the maximum value of the groove-free cutting force. Due to the

presence of grooves, a free surface is provided for the extension of cracks during the cutting process, which reduces the difficulty of rock crushing and is more favorable for cutting stability. The mean feed force data were fitted, as shown in Fig. 17. With increasing cutting depth, the feed force tends to increase linearly, and the feed force of the groove-containing rock is smaller than that of the groove-free rock at the same cutting depth. At a cutting depth of 6-9 mm, the feed force growth is flat; at a cutting depth of 9-12 mm, the feed force growth rate is faster; and at a cutting depth of 12-15 mm, the

feed force growth rate decreases. This is because when the cutting depth is shallow, the spalled rock being cut is closer to both the upper free surface and the free surface of the groove, and at the same time, it is easier for the crack to extend to the free surfaces on both sides so that the rock can be completely crushed under less stress; when the cutting depth increases, the pick tip position is farther from the upper surface, and it is more difficult for the crack to extend to the free surface; only the groove free surface affects the cutting, and the cutting force grows rapidly.

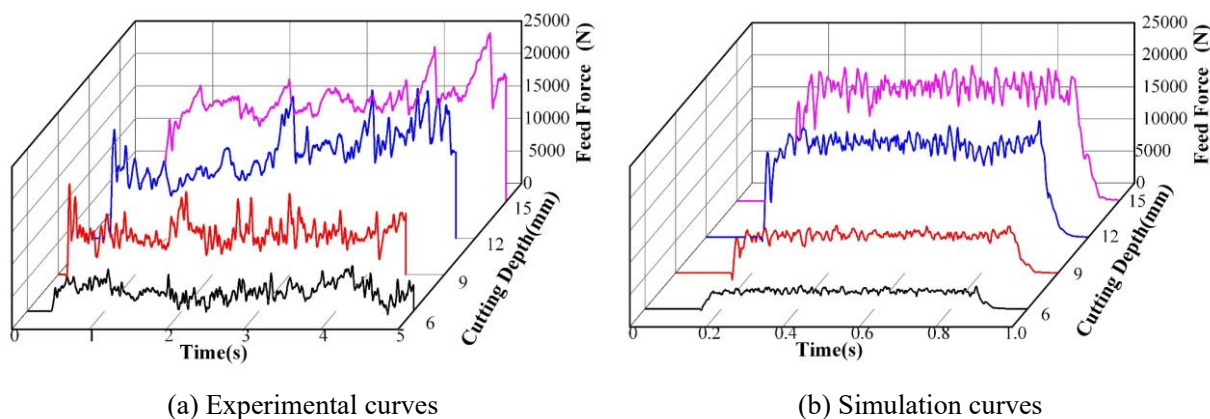


Fig. 16. Cutting force curves for groove-containing rocks with different cutting depths.

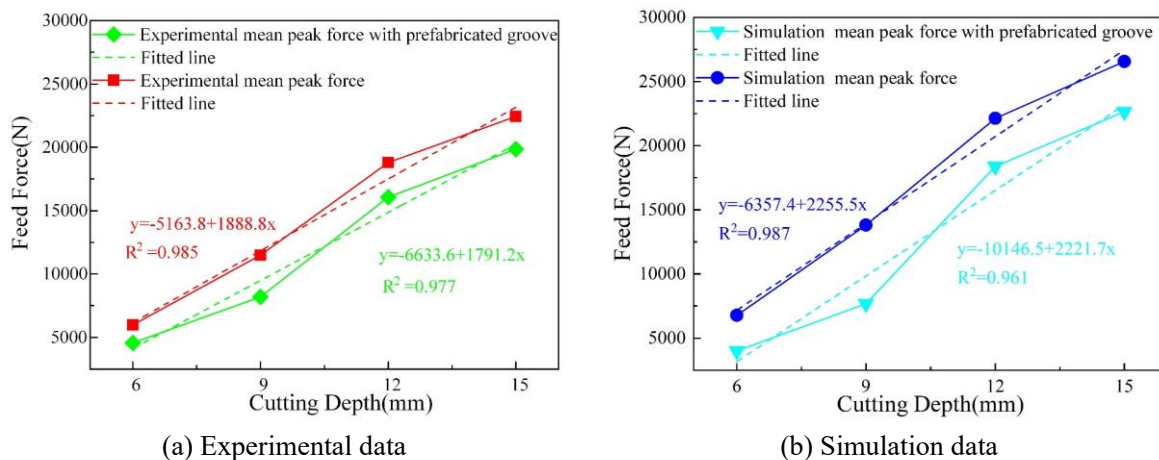
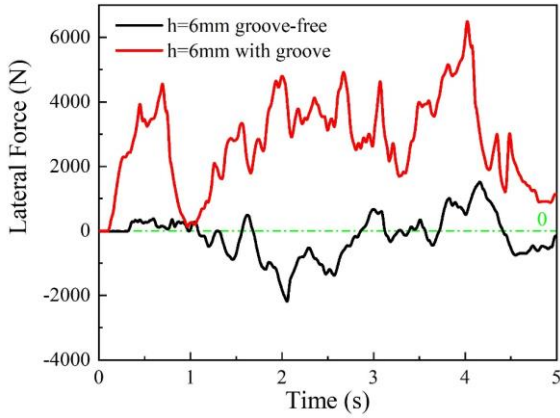


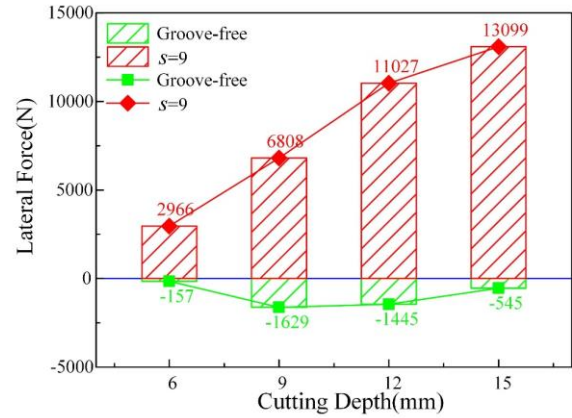
Fig. 17. Comparison of cutting force statistics with and without grooves.

Fig. 18 (a) shows the lateral force curve for a cutting depth of 6 mm, where the lateral force of the groove-free rock fluctuates above and below the 0 scale with a maximum peak size of 2300 N. The lateral force is skewed toward the groove side with a maximum peak of up to 6600 N. Fig. 18 (b) shows the statistical comparison of the mean lateral force at different cutting depths. The mean lateral force of the groove-free rock increases gradually with increasing cutting depth, and the amplitude also increases, but the lateral force of the groove-free rock is more balanced, and the mean value is close to zero. This

is because one side of the pick tip is solid rock during the cutting process of rock containing prefabricated grooves, and on the other side, there exists a free surface provided by the groove, which is much lower than the strength of the rock on the other side, resulting in the lateral forces during the cutting process shifting to the side of the groove; this is one of the most important reasons for the large amount of rock debris on the side of the groove. As the cutting depth increases, the distance of crack extension to the upper free surface gradually increases, the cutting difficulty increases, and the lateral force increases.



(a) Lateral force curves ( $h=12$  mm)



(b) Average values of lateral forces

Fig. 18. Statistical comparison of lateral force curves.

#### 4. Analysis and Discussion of the Specific Energy Consumption

The cutting specific energy consumption refers to the energy consumed by cutting and crushing a unit of rock, which is an important index for evaluating the dynamic crushing process of rock and the efficiency of mechanical rock breaking in the cutting process, and its calculation method is shown in Equation (8).

$$SE = \frac{W}{V} \quad (8)$$

where  $SE$  is the specific energy consumption of cutting, kWh/m<sup>3</sup>;  $W$  is the energy of mechanical work in the cutting process, kWh; and  $V$  is the volume of stripped rock, m<sup>3</sup>.

During the test, the total work performed in the cutting process can be determined by the average force in the cutting process and the cutting distance, and the volume of stripped rock can be determined by the weight of the stripped rock and the density of the rock, while the density of the rock can be determined by the weight of the whole rock and the volume of the rock. Therefore, the cutting specific energy consumption can be converted from Equation (8) to Equation (9) for calculation.

$$SE = \frac{m_z F_m l}{m V_z} \quad (9)$$

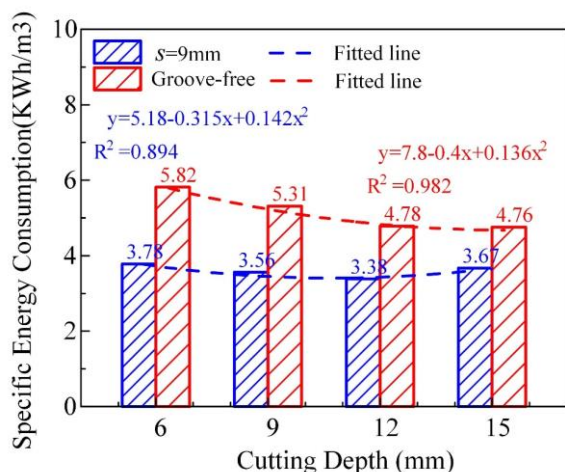
where  $m$  is the mass of the stripped rock, kg;  $F_m$  is the average feed force, kN;  $l$  is the cutting length, m;  $m_z$  is the mass of the whole rock, kg; and  $V_z$  is the volume of the whole rock, m<sup>3</sup>.

Before the experiment, the uncut rock was weighed, and after the experiment, the rock debris produced by cutting was cleaned, weighed and compared with the weight of the rock before the test to determine the specific energy consumption.

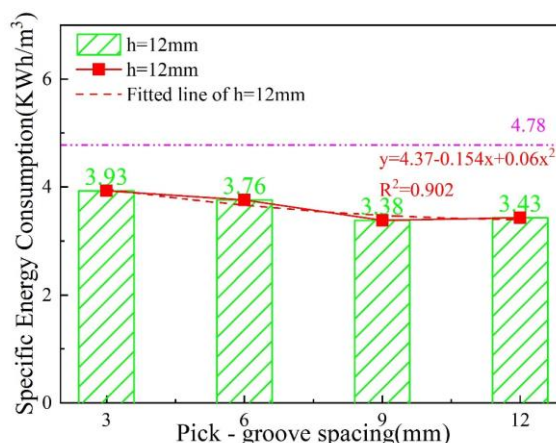
Fig. 19 shows the statistical graph of the specific energy consumption of cutting under different cutting conditions. The specific energy consumption of cutting decreases and then increases with increasing cutting depth, showing a quadratic relationship, and the specific energy consumption is lowest at a cutting depth of approximately 12 mm. This is because when the cutting depth is small, the cutting force required to break the rock is small, the rock debris block size is also small, and the specific energy consumption is high. When the cutting depth is very deep, the conical pick has more difficulty crushing the rock, the cutting force required to crush the rock is large, the cutting stability is poor, part of the crack cannot be extended to the free surface of the situation, and the cutting energy cannot be fully utilized. When the conical pick–groove spacing was 9 mm and the cutting depth was  $h=6$  mm,  $h=9$  mm,  $h=12$  mm, and  $h=15$  mm, the specific energy consumption of the groove-containing rocks decreased by 35.00%, 32.96%, 29.93%, and 22.90%, respectively, compared with that of the groove-free rocks; at a cutting depth of 12 mm, the cutting specific energy consumption of the conical picks with groove spacings of  $s=3$ ,  $s=6$ ,  $s=9$ , and  $s=12$  mm decreased by 17.78%, 21.34%, 29.93%, and 28.82%, respectively, compared with that of the groove-free rocks with the minimum specific energy consumption at  $s=9$  mm. The prefabricated grooves provide a new free surface for the cracks generated during rock crushing, which promotes the extension of the cracks and facilitates the utilization of rock crushing energy. The existence of grooves not only reduces the cutting load during cutting but also reduces the energy consumed by cutting and improves the rock crushing efficiency and the stability of the cutting equipment. In practice, the choice

of the appropriate pick-groove spacing and cutting depth should be based on the working conditions of the project to ensure the

reliability of the equipment while also considering the cutting specific energy consumption.



(a)  $s=9$  mm



(b)  $h=12$  mm

Fig. 19. Comparison of cutting specific energy consumption statistics.

## 5. Conclusions

To reduce the cutting load during the crushing of hard rock by roadheaders, reduce the wear of conical picks, and improve the reliability of the equipment, a conical pick rock-breaking test bed was built to study the load characteristics of conical picks and the rock crushing state during the rock crushing process. Through the finite element analysis method, the stress distribution state of the rock in the breaking process was obtained, and the crushing process of the rock under the cutting action of the conical pick was analyzed. By changing the cutting depth and pick-groove spacing of groove-containing rocks and comparing and analyzing them with groove-free rocks, the change curves of the cutting force of conical picks, the state of the rock stress distribution, and the distribution of the cutting specific energy consumption were obtained. The main conclusions are as follows:

(1) In the process of cutting groove-free rock with a conical pick, a stress concentration is generated at the tip of the pick, and with increasing cutting depth, the feed force shows an increasing trend and has a strong linear relationship, the fluctuation of the feed force increases, the stress area of the rock increases, the crushing area increases, and the rock chip block size increases while the number of rock chips decreases. The cutting forces for grooved rock are lower than those for groove-free rock. Increasing the free surface of rock with prefabricated grooves can effectively reduce the cutting load, which provides

a new way to reduce the wear of conical picks and improve the roadheader operation reliability.

(2) When cutting groove-containing rock, the debris and lateral force are biased to the side of the groove. With increasing conical pick-groove spacing, the rock debris increases, and the feed force increases with a small amplitude. At  $s=12$  mm, the average feed force is 13826 N, and the lateral force increases and then decreases and reaches a maximum value of 10809 N at  $s=9$  mm. When the spacing is unchanged, the cutting force is directly proportional to the cutting depth, and the average value is 17658 N at  $h=15$  mm. The rock debris lumpiness and rock crushing area increase with increasing cutting depth, the lateral force also increases gradually, reaching 13099 N at  $h=15$  mm. Cutting parameters such as the conical pick-groove spacing and cutting depth have a significant effect on the rock-cutting load characteristics, which is a key factor affecting the reliability of roadheaders.

(3) The specific energy consumption of cutting was quadratically related to the cutting depth and pick-groove spacing, and the specific energy consumption of cutting for groove-containing rocks was smaller than that for groove-free rocks. Under the optimal conditions of specific energy consumption,  $h=12$  mm and  $s=9$  mm, the specific energy consumption was 3.38 kWh/m<sup>3</sup>, which was 29.93% lower than that of groove-free rock at  $h=12$  mm. In the actual rock-breaking process, prefabricated rock grooves should be reasonably used according to the working conditions, and an appropriate cutting

depth and conical pick–groove spacing should be selected to ensure the rock-breaking efficiency while considering the

energy consumption of cutting to improve the working reliability of the cutting roadheader.

## Reference

1. Guo D, Song Z, Liu N, Xu T, Wang X, Zhang Y, et al. Performance Study of Hard Rock Cantilever Roadheader Based on PCA and DBN. *Rock Mechanics and Rock Engineering*. 2024;57(4):2605-2623. <https://doi.org/10.1007/s00603-023-03698-1>
2. Zhang X, Li X, Xu W, Gao K, Jiang K, Wang X, et al. Experimental investigation of the failure of conical picks under thermal and abrasive effects. *Engineering Failure Analysis*. 2024;156:107737. <https://doi.org/10.1016/j.engfailanal.2023.107737>
3. Su O, Akkaş M. Assessment of pick wear based on the field performance of two transverse type roadheaders: a case study from Amasra coalfield. *Bulletin of Engineering Geology and the Environment*. 2020;79(5):2499-2512. <https://doi.org/10.1007/s10064-019-01712-x>
4. Liu S, Ji H, Liu X, Jiang H. Experimental research on wear of conical pick interacting with coal-rock. *Engineering Failure Analysis*. 2017;74:172-187. <https://doi.org/10.1016/j.engfailanal.2017.01.013>
5. Zhao G, Jin X, Zhao L, Zhou W, Liu X. Experimental and numerical evaluation for drum dynamic reliability under extremely complex working conditions. *Scientific Reports*. 2024;14(1):642. <https://doi.org/10.1038/s41598-024-51266-6>
6. Praetzas C, Teppernegg T, Mayr J, Czettel C, Schäfer J, Abele E. Investigation of Tool Core Temperature and Mechanical Tool Load in Milling of Ti6Al4V. *Procedia CIRP*. 2018;77:118-121. <https://doi.org/10.1016/j.procir.2018.08.240>
7. Liu X, Tang P, Geng Q, Li X, Tian M. Numerical research on wear mechanisms of conical cutters based on rock stress state. *Engineering Failure Analysis*. 2019;97:274-287. <https://doi.org/10.1016/j.engfailanal.2019.01.045>
8. Li HS, Liu SY, Xu PP. Numerical simulation on interaction stress analysis of rock with conical picks. *Tunnelling and Underground Space Technology*. 2019;85:231-242. <https://doi.org/10.1016/j.tust.2018.12.014>
9. Zhang X, Jiang H, Tian M, Li H, Chen H. Rock cutting performance and wear characteristics of undercutting disc cutter: Based on experiment and DEM. *Wear*. 2023;528-529:204976. <https://doi.org/10.1016/j.wear.2023.204976>
10. Sun R, Mo J, Zhang M, Su Y, Zhou Z. Cutting performance and contact behavior of partial-wear TBM disc cutters: A laboratory scale investigation. *Engineering Failure Analysis*. 2022;137:106253. <https://doi.org/10.1016/j.engfailanal.2022.106253>
11. Dogruoz C, Bolukbasi N, Rostami J, Acar C. An Experimental Study of Cutting Performances of Worn Picks. *Rock Mechanics and Rock Engineering*. 2016;49(1):213-224. <https://doi.org/10.1007/s00603-015-0734-x>
12. Wang Z, Zeng Q, Wan L, Lu Z, Wang H. Investigation of the Influence of Cutting Parameters on Conical Pick Cutting Performance and Rock Damage. *Machines* [Internet]. 2022; 10(11):[1034 p.]. <https://doi.org/10.3390/machines10111034>
13. Wang X, Su O, Wang Q-F, Liang Y-P. Effect of cutting depth and line spacing on the cuttability behavior of sandstones by conical picks. *Arabian Journal of Geosciences*. 2017;10(23):525. <https://doi.org/10.1007/s12517-017-3307-3>
14. Jiang H, Cai Z, Zhao H. Numerical study of hard rock breakage under indenter impact by the hybrid FDEM. *Engineering Fracture Mechanics*. 2020;233:107068. <https://doi.org/10.1016/j.engfracmech.2020.107068>
15. Jiang H, Cai Z, Wang O, Meng D. Experimental and Numerical Investigation of Hard Rock Breakage by Indenter Impact. *Shock and Vibration*. 2020;2020:2747830. <https://doi.org/10.1155/2020/2747830>
16. Li M, Han B, Zhang S, Song L, He Q. Numerical simulation and experimental investigation on fracture mechanism of granite by laser irradiation. *Optics & Laser Technology*. 2018;106:52-60. <https://doi.org/10.1016/j.optlastec.2018.03.016>
17. Guo C, Sun Y, Yue H, Li Q, He S, Zhang J, et al. Experimental research on laser thermal rock breaking and optimization of the process parameters. *International Journal of Rock Mechanics and Mining Sciences*. 2022;160:105251. <https://doi.org/10.1016/j.ijrmms.2022.105251>
18. Zhu X, Luo Y, Liu W. On the rock-breaking mechanism of plasma channel drilling technology. *Journal of Petroleum Science and Engineering*. 2020;194:107356. <https://doi.org/10.1016/j.petrol.2020.107356>
19. Wen S, Du L, Kong Q, Zhang M, Ding X. Study on Microwave-assisted TBM Double-edged Cutter Rock-breaking Efficiency and its Positional Relationship. *Eksplatacja i Niezawodność – Maintenance and Reliability*. 2024;26(2). <https://doi.org/10.17531/ein/186447>
20. Yang H, Lin H, Wang Y, Cao R, Li J, Zhao Y. Investigation of the correlation between crack propagation process and the peak strength for the specimen containing a single pre-existing flaw made of rock-like material. *Archives of Civil and Mechanical Engineering*.

2021;21(2):68. <https://doi.org/10.1007/s43452-021-00175-w>

21. Ping Q, Wang S, Wu Y, Sun S, Shen K, Wang C, et al. Study on Mechanical Properties and Energy Consumption of Fissured Sandstone with Different Dip Angles under Impact Load. *Shock and Vibration*. 2022;2022:5335357. <https://doi.org/10.1155/2022/5335357>
22. Huang Y-H, Yang S-Q, Tian W-L. Crack coalescence behavior of sandstone specimen containing two pre-existing flaws under different confining pressures. *Theoretical and Applied Fracture Mechanics*. 2019;99:118-130. <https://doi.org/10.1016/j.tafmec.2018.11.013>
23. Li Z, Wang L, Li W. Mechanical Behavior and Fracture Characteristics of Rock with Prefabricated Crack under Different Triaxial Stress Conditions. *Minerals* [Internet]. 2022; 12(6):[673 p.]. <https://doi.org/10.3390/min12060673>
24. Li B, Hu M, Zhang B, Li N, Shao W, Nie L, et al. Numerical simulation and experimental studies of rock-breaking methods for pre-grooving-assisted disc cutter. *Bulletin of Engineering Geology and the Environment*. 2022;81(3):90. <https://doi.org/10.1007/s10064-022-02594-2>
25. Wang H, Liao H, He Y, Niu W, Wei J, Niu J, et al. Experimental and numerical simulation study on the effect of granite grooving characteristics on PDC cutter cutting performance. *Geoenergy Science and Engineering*. 2023;230:212256. <https://doi.org/10.1016/j.geoen.2023.212256>
26. Zhang X, Jiang H, Li H, Gu C, Zhao L. Rock fragmentation using the disc tool assisted by the prefabricated kerf: Numerical modelling based on discrete element method (DEM). *Engineering Fracture Mechanics*. 2023;282:109159. <https://doi.org/10.1016/j.engfracmech.2023.109159>
27. Lu Y, Zhang S, He F, Wang L, Wang A, Wang M. Experimental and numerical simulation study on the relationship between cutting depth of high-pressure water jet with high traverse speed and disc cutter penetration of TBM in hard rock tunnel. *Tunnelling and Underground Space Technology*. 2023;142:105387. <https://doi.org/10.1016/j.tust.2023.105387>
28. Ma D-j, Wan L-r, Gao K-d, Zeng Q-l, Wang X-m. The meshing and failure analysis of haulage wheels with the effect by shearer's poses. *Engineering Failure Analysis*. 2022;137:106251. <https://doi.org/10.1016/j.engfailanal.2022.106251>
29. Ma D, Wan L, Zhang X, Zeng Q, Gao K. Meshing characteristics and failure analysis of shearer walking wheel considering torsional deformation. *Alexandria Engineering Journal*. 2022;61(7):5771-5782. <https://doi.org/10.1016/j.aej.2021.09.035>
30. Wang Z, Wang H, Wang J, Tian N. Finite element analyses of constitutive models performance in the simulation of blast-induced rock cracks. *Computers and Geotechnics*. 2021;135:104172. <https://doi.org/10.1016/j.compgeo.2021.104172>